— 26 —

Solar-blind UV detectors based on wide band gap semiconductors

Udo Schühle[I] and Jean-François Hochedez[II]

Abstract

Solid-state photon detectors based on semiconductors other than silicon are not yet considered mature technology but their current development opens new possibilities, also for space observations. Such devices are especially attractive for ultraviolet radiation detection, as semiconductor materials with band gaps larger than that of silicon can be produced and used as "visible-blind" or "solar-blind" detectors that are not affected by daylight. Here we evaluate the advantages of such detectors compared to silicon-based devices and report on the semiconductor detectors that have been fabricated in recent years with materials having large band-gap energies. We describe the most common pixel designs and characterize their general properties.

Wide band gap materials and solar blindness

The present chapter addresses the prospects provided by sensors based on wide band gap materials (henceforth WBG materials or WBGM) as the "active" semiconducting volume. The latter corresponds usually to a solid-state layer where the photons create electron/hole pairs, subsequently collected to produce the signal. WBG materials have also been applied to photo-emissive detectors, e.g., as photocathode coatings on micro-channel plate detectors (Siegmund et al 2003), but in this chapter, we restrict ourselves to solid-state ultraviolet (UV) detection devices made of WBG semiconductors where charge creation and charge collection are taking place inside the material.

One advantage of detectors made of WBG materials is that they can be made "solar-blind". However, solar blindness is a relatively ill-defined concept because it would depend on typical outdoor lighting conditions varying with local time and the Earth's atmosphere. "Visible-blind" UV detectors are required to have a higher responsivity in the UV range than in lower energy ranges. The cut-off of a visible-blind detector is thus at a wavelength shorter than 400 nm. Detectors

[I]MPS—Max-Planck-Institut für Sonnensystemforschung, Katlenburg-Lindau, Germany
[II]ROB—Royal Observatory of Belgium, Brussels; now at LATMOS—Laboratoire Atmosphères, Milieux, Observations Spatiales, Guyancourt, France

with a cut-off below 280 nm could be defined as solar-blind because they respond only to UV radiation with wavelengths shorter than the solar radiation that can penetrate the atmosphere of the Earth. They produce no measurable signal if they are exposed to normal outdoor lighting. In space, the concept of solar blindness would need to be redefined since there is no atmosphere left between the detector and the Sun. It would be appealing to define solar blindness as insensitivity to the solar black-body spectrum. Solar-blind detectors should hence not respond to the FUV, nor photons of lower energy (200 nm to 1220 nm), because the photospheric black-body radiation still prevails in those ranges (cf., Figure 26.1). However, WBG material sensors cannot offer such ideal properties. Real-world solar-blind detectors are sensitive in the VUV (10 nm to 200 nm) or in the XUV (1 nm to 30 nm) ranges, but as little as possible to the MUV (200 nm to 300 nm) and higher wavelengths. To illustrate the above, in Figure 26.1 we relate the quantum efficiency of a diamond photodiode with the solar spectral irradiance as seen from space and from Earth at sea level.

Which are the WBG materials? In case there is no impurity or defect, the minimum photon energy needed to create an electron-hole pair as a signal in the conduction band is associated with the band gap of the material. As the energy of the band gap is thus equal to the energy of the cut-off, we consider the gap between the valence and the conduction bands of the semiconductor to be "wide" if it enables visible-blind detection, that is, if the gap is above ≈ 3.1 eV (400 nm). The WBG materials of interest are C* (diamond), $Al_xGa_{1-x}N$ with all possible stoichiometries from GaN to AlN, BN, ZnS, ZnO, ZnSe, and combinations as, for example, $Al_{1-x}B_xN$. SiC will not be dealt with as it falls short with indirect band gaps at 3.25 eV (4H-SiC), 3.0 eV (6H-SiC), and 2.2 eV (3C-SiC). We focus in the following on GaN (3.4 eV), diamond (5.5 eV), AlN (6.2 eV), and cubic boron nitride (cBN, 6.4 eV).

Actual WBG materials are not ideal by any means. They usually exhibit many crystallographic imperfections influencing the mobility of charge carriers. This requires the artificial synthesis of WBG material layers, because natural substrates are rare and actually inappropriate without certain doping profiles. Although the various techniques for growing epitaxial layers have made immense strides in the recent years, diamond, cBN, AlN, and even GaN must still be acknowledged as relying on new/emerging technology.

Radiation hardness, dark current, and more

A consequence of the large band gap is the reduction of the dark current, permitting room temperature operations. In addition to the improved noise performance, this is a great advantage in terms of sparing the resources (mass and power) needed to cool a subsystem in space. Moreover, it brings the additional benefit of avoiding a cold surface that would trap residual molecules. Not only water can deposit on the cold surface; it is well known that hydrocarbons outgassing from organic materials used in space instrumentation may deposit on the cold detector, and polymerize under UV illumination, leading to irreversible opaque absorbing layers (Schühle 2003). It is therefore highly beneficial to operate UV sensors in warm

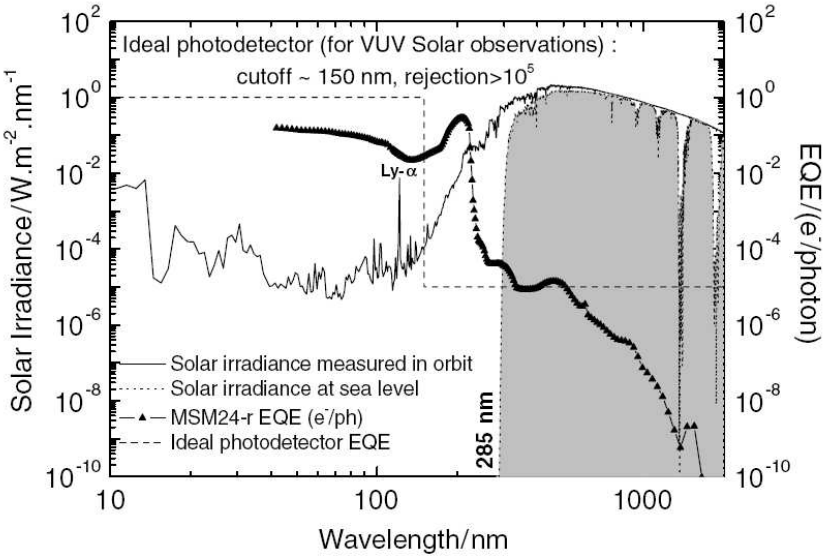

Figure 26.1: The solar spectral irradiance measured in space and from Earth (left ordinate axis) compared with the quantum efficiency (right ordinate axis) of an ideal WBG detector for solar observations and of a real diamond MSM detector (BenMoussa et al 2008b).

conditions.

An additional asset for space applications is radiation hardness (see, e.g., Rahman et al 2004), which is of paramount importance for the lifetime of missions and instruments (Hochedez et al 2003; Schühle et al 2004). The mobility of charge carriers in WBG materials can be very high (C*, GaN). It provides a fast response of detectors and enables high-cadence observations, including new photon-counting readout schemes. To summarize, in Table 26.1 we list the main differences between silicon-based and WBGM-based devices.

Table 26.1: Differences between silicon- and prospective WBGM-based devices.

Silicon-based detectors	WBG-based detectors
Dark current at room temp., need cooling	Lower dark current
Cold trap of contaminants	Less contamination (long-term stable)
Degradation by displacement radiation	Rad-hardness (increased lifetime)
QE evolving and inhomogeneous	QE stable and better flatfield
Minimal pixel size ≈ 5 µm	Sustain higher electrical fields
Need blocking filters to suppress visible	Need fewer blocking filters

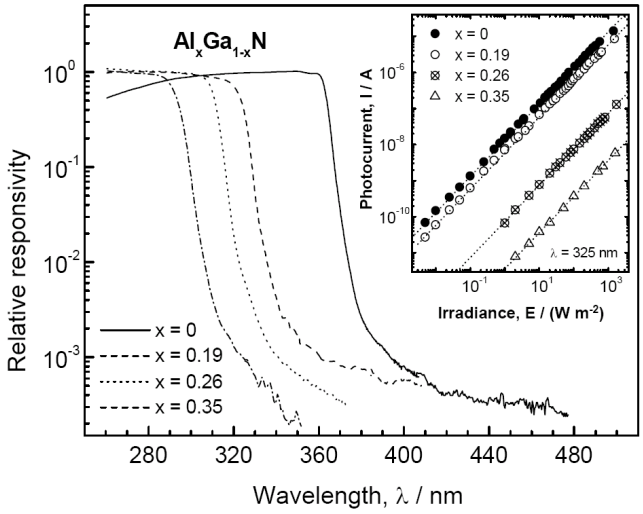

Figure 26.2: Relative responsivity of AlGaN Schottky diodes with different aluminium content at their threshold energies (after Muñoz et al 2001). The insert shows their linearity over three decades of irradiance.

Solutions for WBG materialbased sensors

Most of the WBGM-based devices built so far have been designed specifically for visible-blind UV detection applications. The "Blind to Optical Light Detectors" (BOLD) project has been initiated in 1999 to design and develop diamond, nitride, and other WBGM–based detectors, especially for astrophysics (Hochedez et al 2000). In recent years different designs have been developed, from single-pixel photodiode-type detectors to imaging arrays, based on various WBG materials. In practice, the material can be selected according to the specific requirements of the application.

WBG materials usually have a large penetration depth above the wavelength threshold, and a shallow penetration depth below. This leads to optimal charge collection and therefore to high efficiency in a passband around the band gap. The detector itself serves thereby as a spectral filter. By selecting the material according to the wavelength of application, the detector is most efficient in that given spectral region (see, e.g., BenMoussa et al 2006a and references therein). Devices built from III-V nitrides are promising for a wide range of UV applications, and technological progress has been made with GaN and AlGaN devices (Pearton et al 1999; Monroy et al 2003; Aslam et al 2005). With the band-gap energies of 3.4 eV of GaN and 6.2 eV of AlN it is possible to build UV detectors with precisely selected responsivity thresholds between these energies by selecting the fraction of aluminium in the $Al_xGa_{1-x}N$ alloy material (Muñoz et al 2001; Sandvik et al 2001; Tripathy et al 2007). Figure 26.2 shows as example the relative responsivity of AlGaN devices (Schottky-diodes) with different aluminium content at their threshold energies.

Diamond is another promising WBG material (Collins 2009). Both single-crystal and polycrystalline thin-film diamond devices have been explored as photoconductive detectors. Its band-gap energy of 5.5 eV corresponds to a threshold wavelength of 225 nm. It has been identified as a promising material for solar-blind UV detectors in space environments (McKeag et al 1997)

A possible alternative to diamond is boron nitride (BN) with a band-gap energy of 6.4 eV. Recently, metal-semiconductor-metal (MSM) photoconductors based on cubic BN films have been produced (Soltani et al 2008). The main obstacle in developing UV detectors with WBGM is in producing high-quality material by growing high-purity semiconductor thin film layers with minimal defects and dislocations on the substrate material. Major problems relate to impurities, vacancies, lattice discontinuities, phase boundaries, lattice mismatch with the substrate, and appropriate doping with n- and p-type materials. Many techniques for epitaxial growth are being investigated but their description is beyond the scope of this book.

Pixel architectures – a brief comparative assessment

There are different types of semiconductor detectors, the most important are: photoconductors, MSM diodes, Schottky barrier and p-i-n photodiodes. The schematic structures are depicted in Figure 26.3, using AlGaN as the active WBG semiconductor material. The following subsections provide a brief comparison of performances and limitations. For more details we refer to the review by Razeghi and Rogalski (1996).

Photoconductors: Photoconductors consist of a semiconductor layer with two ohmic contacts and a voltage bias applied between them. Under illumination, the conductance of the semiconductor changes with the intensity of the incident radiation. The current is mainly due to majority charge carriers since they are free to flow across the ohmic contacts. However, the majority carrier current depends on the presence of the minority carriers. The minority carriers pile up at one of the contacts, where they cause additional injection of majority carriers (current continuity and charge conservation) until the minority carriers recombine. This effect can cause large "photoconductive" *gain*, which depends primarily on the ratio of the minority carrier lifetime to the majority carrier transit time. Long carrier lifetimes therefore cause large gain, but also a slow response time. The photoconductive gain is one of the good features of photoconductors. An undesirable attribute of photoconductors is a relatively high dark current. However, photoconductors are simple and useful for those applications where speed and dark current are not particularly important.

MSM photodiodes: The MSM diode is made of two Schottky barrier diodes back-to-back. The entire semiconductor layer between two metal electrodes becomes fully depleted under sufficient bias. The geometric parameters of a conventional MSM photodetector pixel element determine its performance. The device consists of alternating metal contacts deposited on the semiconductor active layer. MSM structures represent a very simple photodetector design. Their main limitations include relatively large dark current (since a bias voltage is required) and

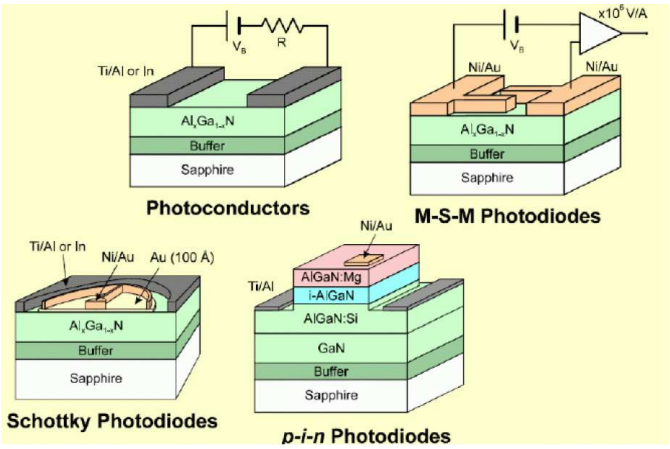

Figure 26.3: Schematic structure of different semiconductor photodetectors (courtesy of E. Muñoz).

somewhat lower external quantum efficiency due to electrode shadowing.[1]

Schottky diodes: Schottky diodes are a good alternative to MSM detectors due to the fact that these detectors can operate in photovoltaic mode, i.e., without bias voltage (and no resulting dark current), and therefore with high signal/noise ratio. A Schottky diode requires an ohmic contact, i.e., a conductive layer like, n-type AlGaN.

Pin photodiodes: The most common form of photodiode used is the pin diode which consists of a p-type, highly doped, transparent contact layer on top of an undoped absorbing layer and an n-type, highly doped contact layer on the bottom. Since there are very few charge carriers in the intrinsic region, the space charge region reaches completely through from the p to the n region. This results in detectors with several important advantages: they are fast, stable, linear and low-noise. The primary disadvantage of the pin diodes is that with moderate doping concentrations in the conducting regions for low resistance, the resulting depletion region is quite thin. This causes two problems:
— low efficiency when little absorption occurs in a thin depletion region, and
— relatively high capacitance which decreases device speed.

A general rule is that only carriers generated within the depletion region are *efficiently and rapidly* collected as photocurrent. The goal is to create a diode with a wide depletion region.[2]

[1]For interdigitated fingers, Au or Al (<10 nm) can be used as EUV semi-transparent contact. Three different approaches to improve the responsivity of MSM detectors are: size reduction towards sub-micrometre fingers, use of semitransparent electrodes, or asymmetric electrodes. All these solutions provide better detector characteristics in terms of dark current, UV/visible contrast, linearity, and responsivity. The shadowing of the active area by the interdigitated contacts is the main drawback of the MSM detector, reducing their efficiency. The spacing-to-width ratio of the fingers is the major parameter that determines the detector's reponsivity.

[2]The material quality is crucial since the optical performance in the EUV is strongly influenced by the surface characteristics (generation of e-h pairs near the surface, dead layer, oxide). A high-quality active layer is required and the thickness for total absorption should be optimised for low

In summary, the preferred type of photosensitive diode for a given application depends on its inherent properties and the choice may depend on various constraints, not only related to performance but also to ease of the fabrication process: photoconductors and Schottky diodes can be built with co-planar structures, making their production simpler than pin diodes which consist of different layers (sandwich-type) with different doping.

In general, photoconductive devices have a high sensitivity and may profit from internal photoelectric gain (in constant voltage operation mode). Since they need a bias voltage, they have low impedance but usually a higher background (dark signal) than Schottky or pin diodes, in which the charge is created by photo effect against an internal potential barrier. The latter provides the advantages of bias-free operation, low background signal, fast response, and better signal stability.

Responsivity

The responsivities reported are quite high just above the band-gap energy, reaching values up to 0.2 AW^{-1}. For example: Parish et al (1999) report on AlGaN pin detectors on laterally epitaxially overgrown GaN with a dark current level of 10 $nAcm^{-2}$ at -5 V bias voltage and a peak responsivity of 0.05 AW^{-1} at 285 nm. Motogaito et al (2001) realized a responsivity of 0.15 AW^{-1} with GaN Schottky diodes. Pau et al (2004) have reported responsitivities of GaN Schottky diodes of 0.03 AW^{-1} and of MSM photoconductors of 0.04 AW^{-1}. The responsivity depends also on the separation of the charge-collecting metal electrodes on the semiconductor surface. The smaller the distance between the metal electrodes, the better is the charge collection. Malinowski et al (2008) show GaN devices (threshold at 370 nm) with a peak responsivity of 0.162 AW^{-1} at 360 nm with a rejection of longer wavelengths of almost four orders of magnitude towards 400 nm. High responsivity can be obtained with avalanche photodiodes using their internal gain with reverse-biased operation. Tut et al (2007) report an internal gain of 1560 with AlGaN photodiodes and a peak responsivity of 0.13 AW^{-1} at 272 nm.

While the efficiency of the devices is highest just above the threshold, at shorter wavelengths, where the penetration depth decreases, the detection of charge carriers is decreased by processes such as surface recombination and photoemission losses (Motogaito et al 2001, BenMoussa et al 2008a), a complication that needs to be carefully addressed in the design of detectors for the VUV range.

Photodetectors based on diamond material could recently progress due to success in producing high-quality thin films with sufficiently low defects and concentrations of n-type and p-type dopants (e.g., Nesladek 2005). The first diamond detectors that ~~will be~~ flown on a space mission ~~will be~~ the detectors of the solar XUV-VUV radiometer LYRA aboard the *PROBA2* satellite (see Figure 26.4, Hochedez et al 2006; BenMoussa et al 2006). LYRA ~~will carry~~ several large area (4.6 mm diameter) diamond diodes which have been especially fabricated for this mission. They have a sufficiently uniform response over their active area and reach a peak responsivity of 0.048 AW^{-1} at 210 nm (BenMoussa et al 2008b).

defects, cracks-free, low roughness, and good structural homogeneity. The doping level of the active layer is also one of the most critical parameters and should be below 10^{16} cm^{-3} in order to achieve a depletion reach-through region for reasonable electrode gap spacing.

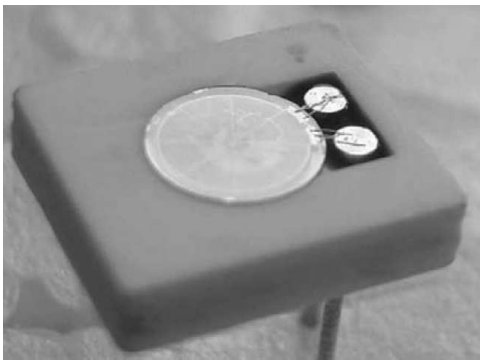

Figure 26.4: Diamond MSM photodiode of the LYRA EUV radiometer aboard *PROBA2* (courtesy A. BenMoussa).

Imaging arrays and hybridization

We distinguish two technologies for the fabrication of imaging arrays: first, deposition of the active material for charge creation directly on the signal readout integrated circuit (ROIC) and second, hybridization, where the WBG semiconductor array and the silicon-based readout circuitry are developed and fabricated independently to the same pixel scale (pitch) and then bonded to each other. The two arrays are combined by indium bump bonding, which involves flipping one array on the other (flip-chip integration). The definition of indium bumps is presently limiting the miniaturization of pixel size and pitch. Figure 26.5 shows a detail of the indium bump structure processed on a sensor array.

Using this technique, focal plane arrays (FPA) of AlGaN detectors have been produced by several groups, e.g., with 256 × 256 pixels (Lamarre et al 2001; Aslam et al 2005) and 320 × 256 pixels (Long et al 2002; McClintock et al 2005). These devices employ deposition of the array structure on a transparent substrate and illumination from the back side (back-illumination) through the substrate. For shorter wavelengths than the transmission cut-off of the substrate material,however,—in the VUV range—front-side illumination of the device is required. Further in the EUV (below ≈ 30 nm) back-side illumination is again possible with a device that is back-side thinned, making it transparent to the EUV and X-ray radiation ranges.

By ~~deposing~~ the WBG material directly on the readout circuit, the monolithic array fabrication is less technology intensive in principle, since the fabrication can be carried out on one wafer and the flip-chip bonding process is not required. This technique has been applied with infrared-sensitive materials and may offer larger yields of ultraviolet detector arrays in the future.

It is the conviction of the authors that future scientific discoveries rely on new detector developments. The presented progress with WBGMs bears out the prospects for enhanced performance of future missions.

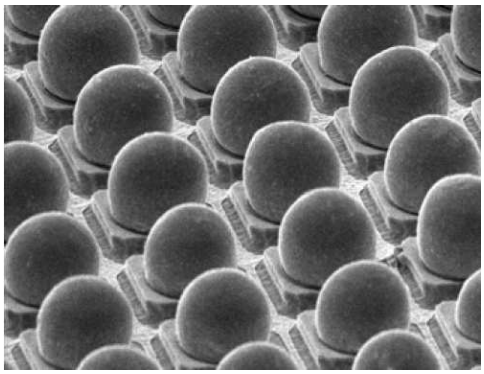

Figure 26.5: Scanning electron microscope (SEM) picture of a detail of a 256 × 256-element sensor array realized in III-V material after the indium bump processing. The pixel pitch is 25 µm (courtesy of IMEC, Belgium).

Acknowledgements

We gratefully acknowledge the contributions to this work by A. BenMoussa and by other colleagues of the BOLD projects.

Bibliography

Aslam S, Yana F, Pugel DE (plus six authors) (2005) Development of ultra-high sensitivity wide-band gap UV-EUV detectors at NASA Goddard Space Flight Center. Proc SPIE 5901:59011J-1–12

BenMoussa A, Schühle U, Scholze F (plus ten authors) (2006a) Radiometric characteristics of new diamond PIN photodiodes. Meas Sci Technol 17: 913–917

BenMoussa A, Hochedez JF, Schühle U (plus 13 authors) (2006b) Diamond detectors for LYRA, the solar VUV radiometer on board PROBA2. Diamond Rel Mat 15:802–806

BenMoussa A, Hochedez JF, Dahal R (plus seven authors) (2008a) Characterization of AlN metal-semiconductor-metal diodes in the spectral range of 44–360 nm: Photoemission assessments. Appl Phys Lett 92:0221081–0221083

BenMoussa A, Soltani A, Haenen K (plus eight authors) (2008b) New developments on diamond photodetector for VUV solar observations. Semicond Sci Technol 23:0350261–0350267

Collins AT (2009) Detectors for UV and far UV radiation. In: CVD diamond for electronic devices and sensors. Sussmann RS (Ed.):165–183 John Wiley & Sons, Chichester UK

Hochedez JF, Verwichte E, Bergonzo P (plus eight authors) (2000) Future diamond UV imagers for solar physics. Phys Stat Sol A 181:141–149

Hochedez JF, Schühle U, Pau JL (plus 23 authors) (2003) New UV detectors for solar observations. Proc SPIE 4853:419–426

Lamarre P, Hairston A, Tobin S (plus 13 authors) (2001) AlGaN p-i-n photodiode arrays for solar-blind applications. Phys Stat Sol A 188:289–292

Long JP, Varadaraajan S, Matthews J, Schetzina JF (2002) UV detectors and

focal plane array imagers based on AlGaN p-i-n photodiodes. Opto-Electr Rev 10:251–260

Malinowski P, John J, Lorenz A (and 13 authors) (2008) AlGaN photodetectors for applications in the extreme ultraviolet (EUV) wavelength range. Proc SPIE 7003A: 70030N1–70030N8

McClintock R, Mayes K, Yasan A (plus three authors) (2005) 320 × 256 solar-blind focal plane arrays based on $Al_xGa_{1-x}N$. Appl Phys Lett 86:0111171–0111173

McKeag RD, Marshall RD, Baral B (plus two authors) (1997) Photoconductive properties of thin film diamond. Diamond and Related materials 6:374–380

Monroy E, Omnès F, Calle F (2003) Wide-band gap semiconductor ultraviolet photodetectors. Semiconductor Science and Technology 18:R33–R51

Motogaito A, Ohta K, Hiramatsu K (plus four authors) (2001) Characterization of GaN based UV-VUV detectors in the range 3.4–25 eV by using synchrotron radiation. Phys Stat Sol A 188:337-340

Muñoz E, Monroy E, Pau JL (plus three authors) (2001) III nitrides and UV detection. J Phys Condens Matter 13:7115–7137

Nesladek M (2005) Conventional n-type doping in diamond: state of the art and recent progress. Semicond Sci Technol 20:R19–R27

Parish G, Keller S, Kozodoy P (plus seven authors) (1999) High-performance (Al,Ga)N-based solar-blind ultraviolet p-i-n detectors on laterally epitaxially overgrown GaN. Appl Phys Lett 75:247–249

Pau JL, Rivera C, Muñoz E (plus six authors) (2004) Response of ultra-low dislocation density GaN photodetectors in the near- and vacuum-ultraviolet. J Appl Phys 95:8275–8279

Pearton SJ, Zolper JC, Shul RJ, Ren F (1999) GaN: Processing, defects, and devices. J Appl Phys 86:1–78

Rahman M, Al-Ajili A, Bates R (plus 14 authors) (2004) Super-radiation hard detector technologies: 3-D and widegap detectors. IEEE Trans Nucl Sci:2256–2261

Razeghi M, Rogalski A (1996) Semiconductor ultraviolet detectors. J Appl Phys 79:7433–7473

Sandvik P, Mi K, Shahedipour F (plus four authors) (2001) $Al_xGa_{1-x}N$ for solar-blind UV detectors. J Crystal Growth 231:366–370

Schühle U (2003) Cleanliness and calibration stability of UV instruments on *SOHO*. Proc SPIE 4853:88–97

Schühle U, Hochedez JF, Pau JL (plus 18 authors) (2004) Development of imaging arrays for solar UV observations based on wide band gap materials. Proc SPIE 5171:231–238

Siegmund OHW, Tremsin A, Martin A (plus three authors) (2003) GaN photocathodes for UV detection and imaging. Proc SPIE 5164:134–143

Soltani A, Barkad HA, Mattalah M (plus nine authors) (2008) 193 nm deep-ultraviolet solar-blind cubic boron nitride based photodetectors. Appl Phys Lett 92:0535011–0535013

Tripathi N, Grandusky JR, Jindal V, (plus two authors) (2007) AlGaN based tunable hyperspectral detector. Appl Phys Lett 90:2311031–2311033

Tut T, Gokkavas M, Inal A, Ozbay E (2007) $Al_xGa_{1-x}N$-based avalanche photodiodes with high reproducible avalanche gain. Appl Phys Lett 90:1635061–1635063